Edinburgh Research Explorer

Tacticity Control in the Synthesis of Poly(lactic acid) Polymer Stars with Dipentaerythritol Cores

.

Tacticity Control in the Synthesis of Poly(lactic acid) Polymer Stars with Dipentaerythritol Cores**

Michael P. Shaver[1],* and Donald J. A. Cameron[1]

[1]Department of Chemistry, University of Prince Edward Island, 550 University Avenue, Charlottetown, PE, C1A 4P3, Canada.

[*]Corresponding author; e-mail: mshaver@upei.ca (current address: Michael.Shaver@ed.ac.uk, EaStCHEM, School of Chemistry, Joseph Black Building, University of Edinburgh, West Mains Road, Edinburgh, EH9 3JJ, UK).

Graphical abstract:

[M] controls polymer tacticity, physical properties and hydrolytic degradation
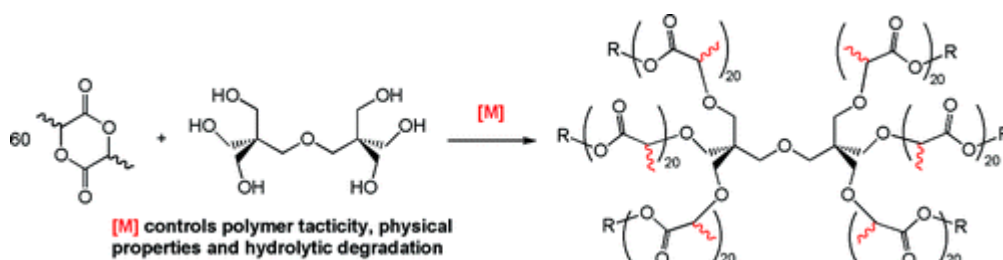
Abstract

The synthesis of a family of polymer stars with arms of varied tacticities is discussed. The effect of polymer tacticity on the physical properties of these polymer stars is presented. Dipentaerythritol cores support six poly(lactic acid) (PLA) arms. Lewis acidic tin and aluminum catalysts control the polymerization to afford polymer stars of variable tacticity. The analysis of these polymers by NMR spectroscopy, thermogravimetric analysis, powder X-ray diffraction, and differential scanning calorimetry reveals the effects of tacticity control on the physical properties of the polymer stars. Preliminary decomposition studies suggest that the biodegradation profile of a polymer star may also be tuned by stereochemical control. This is the first systematic altering of tacticity in PLA polymer stars, showing that polymer tacticity can have a great impact on star properties.

Introduction

Research into the synthesis and applications of biodegradable aliphatic poly(esters) including poly(ε-caprolactone), poly(glycolic acid), and poly(lactic acid) (PLA) and their copolymers continues to grow. The renewable, bioassimilable, and biodegradable nature of these materials has expanded applications in biomedical, pharmacological, and environmental fields.[1] In particular, PLA has received an extensive amount of interest from both academic and industrial researchers, especially in biological applications, where it has seen application in surgical sutures,[2] tissue engineering,[3] and drug delivery systems.[4] The controlled synthesis of PLA is accomplished through the ring-opening polymerization (ROP) of lactide, the cyclic diester of lactic acid.[5] Because the lactide monomer possesses two stereocenters, three distinct diastereomers exist: dd-, ll-, and dl-lactide. The enantiopure isomers have been the focus for the aforementioned studies, as both single enantiomers or a racemic mixture (*rac*-lactide). However, challenges exist in the application of linear chains of PLA in biomedical and pharmacological applications because in vitro and in vivo degradation rates are often not controlled, bioactive loading is low, and products have a high hydrophobicity.[6, 7]

One method to overcome these deficiencies has been to incorporate lactide monomer units into star- or comb-shaped polymers possessing unique physicochemical properties.[8, 9] These materials can have high molecular weights while maintaining relatively short PLA chains, resulting in a higher hydrophilicity and improved degradation profiles.[10-12] Early PLA polymer stars utilized multifunctional initiators including sugar alcohols,[13-15] poly(saccharide)s,[16] and poly(vinyl alcohol).[17] This "core first" approach forms star-shaped polymers bearing strictly defined numbers of linear arms. A recent focus has been the preparation of polymer stars with pentaerythritol (PE)[18-25] and dipentaerythritol (DPE)[7, 25-27] cores to produce four- and six-armed polymer stars, respectively. These polymer stars are traditionally prepared in bulk l-lactide or *rac*-lactide at 125 °C using tin(II) ethylhexanoate (stannous octanoate, Sn(Oct)$_2$) as a catalyst. The novel PE- and DPE-

derived macrostructures have shown utility in controlled drug release,[28] nanoparticle synthesis,[7] and micelle formation.[29]

Whereas extensive work has been carried out on varying the polymer core, chain length, and (co)monomers in these polymer macrostructures, little effort has been spent on understanding the relationship between polymer microstructure and macrostructure. Specifically, there remains a divide between the catalyst development and mechanistic work on the stereocontrolled ROP of lactide and the fields of polymeric drug delivery systems and polymer macrostructure synthesis. Studies with a Sn(Oct)$_2$ catalyst are limited to two polymer tacticities: if *rac*-LA is used as a feedstock, then an atactic polymer chain is produced, whereas if enantiopure l-LA is used, then an isotactic l-PLA is synthesized. However, polymers of variable tacticity can be produced directly from the inexpensive *rac*-LA with judicious choice of catalyst (Figure 1).[5] Catalyst development in this area has been especially broad, with stereocontrolled ROP reported for Al-, Ca-, Ge-, Hf-, In-, La-, Li-, Mg-, Nd-, Sc-, Sm-, Sn-, Ti-, Y-, Zn-, and Zr-based catalysts,[5] but application of this work to polymer stars has been minimal. The preparation of stereocomplex polymer stars from the combination of independently prepared d- and l-lactide polymer stars, catalyzed by Sn(Oct)$_2$, has been reported to give materials with increased melt stability,[27] although polymers exhibiting stereocomplex properties can be prepared from *rac*-LA using mixtures of enantioselective catalysts. Whereas a heterotactic six-armed polymer star was prepared by utilizing an aluminum catalyst and evaluated as part of a larger study examining the one-pot preparation of α-ω-chain end-functionalized PLA,[26] our report represents the first systematic investigation of the effect of catalyst and tacticity on the physical properties of PLA polymer stars.
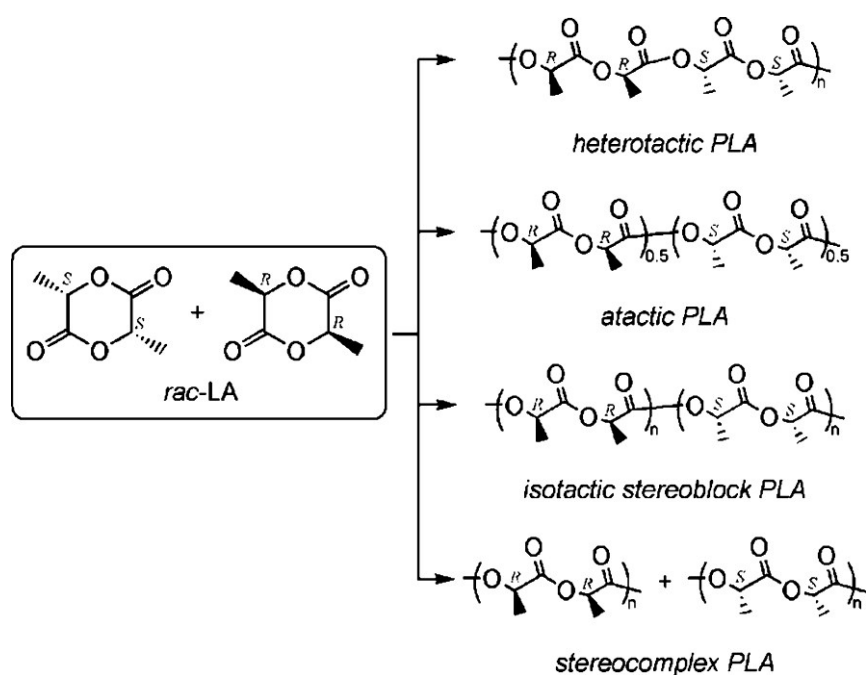

Figure 1. PLA microstructures from the stereocontrolled ROP of *rac*-lactide.

We report the synthesis of a series of six-armed polymer stars of variable tacticity built on a core molecule of DPE. Tin and aluminum catalysts allow for polymer arms with atactic, heterotactic, and isotactic biases to be synthesized. Characterization of these materials using gel permeation chromatography (GPC), ^{1}H NMR spectroscopy, thermogravimetric analysis (TGA), powder X-ray diffraction (p-XRD), and differential scanning calorimetry (DSC) allows us to observe the interplay between microstructure and macrostructure control in these systems, indicating that some polymer characteristics can be controlled by judicious choice of catalyst. Additionally, preliminary biodegradation studies are also reported and linked to polymer microstructure. In this Article, we show that the effect of tacticity on the properties of polymer stars is significant. Whereas this work is based on synthetic novelty, as the introduction of all of the known tacticities available from *rac*- and l-lactide into polymer star architectures has been previously unreported, the impact may be found in the use of stereocontrol to modify significantly star polymer properties.

Experimental Section

Materials

HPLC-grade acetone, acetonitrile, dichloromethane, ethanol, methanol, and toluene were purchased from Fisher Scientific, whereas deuterated solvents were purchased from Cambridge Isotopes. We dried acetonitrile by stirring the solvent over calcium hydride for 48 h, distilling under a dinitrogen atmosphere, and thoroughly degassing the anhydrous solvent. We obtained anhydrous toluene by passing the solvent through an Innovative Technologies solvent purification system consisting of columns of alumina and a copper catalyst. Anhydrous solvents were tested with the addition of a toluene solution of sodium benzophenone ketyl prior to use. Deuterated solvents were dried in analogous procedures, then trap-to-trap distilled and freeze−pump−thaw degassed three times. Chemicals for catalyst synthesis, including trimethyl aluminum (2.0 M solution in hexanes), 2,4-dichlorophenol, *N,N′*-dibenzylethylenediamine, paraformaldehyde, 3,5-di-*tert*-butyl-2-hydroxybenzaldehyde, 1,2-diaminoethane, and tin(II) ethylhexanoate were purchased from Aldrich Chemical and used as received. DPE was purchased from Aldrich Chemical and purified by recrystallization from methanol and dried in a desiccator for 48 h prior to use. The monomers *rac*- and l-lactide were purchased from PURAC Biomaterials and purified by three successive vacuum sublimations of the material prior to use. 1,5,7-Triazabicyclo[4,4,0]dec-5-ene was purchased from Aldrich Chemical and used as received. The aluminum catalysts [tBu][salen]AlMe (**1**), where [tBu][salen] is *N,N′*-ethylenebis(3,5-di(*tert*-butyl)salicylimine), and [Cl][salan]AlMe (**2**), where [Cl][salan] is *N,N′*-ethylenebis(benzyl)(bis(3,5-dichlorosalicylamine), were synthesized by following previously reported procedures.[30, 31]

General Considerations

All experiments involving moisture and air-sensitive compounds and catalysts were performed under a nitrogen atmosphere using an MBraun LABmaster sp glovebox system equipped with a −33 °C freezer and [H_2O] and [O_2] analyzers. GPC was carried out in THF (flow rate: 1 mL min^{-1}) at 50 °C with a Polymer Laboratories PL-GPC 50 Plus integrated GPC system using three 300 × 7.5 mm Resipore columns. Polystyrene standards were used for calibration and corrected for PLA. ^{1}H NMR and 2-D spectra were recorded with a Bruker Avance Spectrometer (300 MHz) in CDCl$_3$, CD$_3$OH, or C$_6$D$_6$. Elemental analyses were conducted by Guelph Analytical Laboratories. Thermogravimetric analysis was performed on a TA Instruments TGA Q500 under an inert nitrogen atmosphere with a flow rate of 60 mL min^{-1} and a heating rate of 10 °C min^{-1}. DSC was performed on a TA Instruments DSC Q100 using a heating rate of 10 °C min^{-1}. p-XRD was performed on a Bruker AXS D8 Advance diffractometer equipped with a graphite monochromator, variable divergence, and antiscatter slits and a scintillation detector. Cu Kα radiation (λ = 1.542 Å) was used, and data collection was carried out in air, at room temperature, using a scan range of 2−60°. Solid samples were pressed as thin pellets and run on a nondiffracting silicon substrate.

Polymerization Experiments

All polymerization reactions were performed in sealed ampules under an inert atmosphere, at 120 °C, with a molar ratio of monomer/catalyst/alcohol functionality of 60:1.2:1. Catalysts employed included ^{tBu}[salen]AlMe (**1**), ^{Cl}[salan]AlMe (**2**), and Sn(Oct)$_2$ (**3**). Monomers employed included *rac*-lactide and l-lactide, whereas the initiator molecule was either benzyl alcohol or DPE. The reaction proceeded for the allotted period of time required to reach 90% conversion and was then quenched with a 10:1 v/v solution of either CH$_2$Cl$_2$/MeOH or CH$_2$Cl$_2$/PhCH$_2$OH for 30 min at room temperature to form hydroxy-terminated polymer chains. The resulting mixture was precipitated from cold methanol, collected via filtration, and dried in vacuo prior to analysis.

For example, *rac*-lactide (0.500 g, 3.52 mmol), DPE (0.0148 g, 0.0587 mmol), and **1** (0.0384 g, 0.0704 mmol) were added to an ampule equipped with a magnetic stirring bar in the glovebox. The ampule was sealed and placed in a preheated oil bath at 120 °C for 6 h. The ampule was removed from the oil bath, cooled to room temperature, opened to the atmosphere, and quenched with 10 mL of a 10:1 v/v solution of CH$_2$Cl$_2$ and methanol. The solution was stirred for 30 min and then added dropwise to 100 mL of cold methanol to precipitate the polymer. The resultant white polymer was collected via filtration and dried in vacuo for 12 h. Monomer conversion was determined gravimetrically to be 92% (0.474 g).

Degradation Experiments

PLA star polymer samples (200.0 mg) were pressed into thin pellets and suspended in 5.0 mL of a 0.05% weight/volume solution of 1,5,7-triaza-bicyclo[4.4.0]dec-5-ene (TBD) in methanol in a 25 mL scintillation vial. The solutions were agitated at 23 °C until degradation was complete and the time to complete degradation was recorded. Degradation of the materials was confirmed by GPC and NMR spectroscopy. Experiments were performed in quadruplicate to ensure the integrity of the results.

Results and Discussion

Synthesis and Characterization of Tacticity Controlled Polymer Stars

Extensive work on aluminum catalysts supported by salan[30] and salen[31] tetradentate ligands has provided excellent control over the tacticity of linear PLA polymer chains. In particular, catalysts **1** and **2** in Figure 2 provide for >90% isotactic and heterotactic linkages, respectively. This contrasts greatly with the catalyst traditionally used in commercial synthesis of this polymer because catalyst **3** synthesizes PLA with a random, atactic bias when utilizing *rac*-lactide as monomer. The effect of this polymerization stereocontrol is well-documented for linear PLA chains, with stereoregular PLAs exhibiting variable crystallinity, melt temperature (T_m), and degradation rate of the polymer depending on the polymer tacticity.[5, 32-34] Systematic extension of this tacticity control to branched and hyperbranched PLA macromolecules remains underexplored, especially in the field of PLA polymer stars.
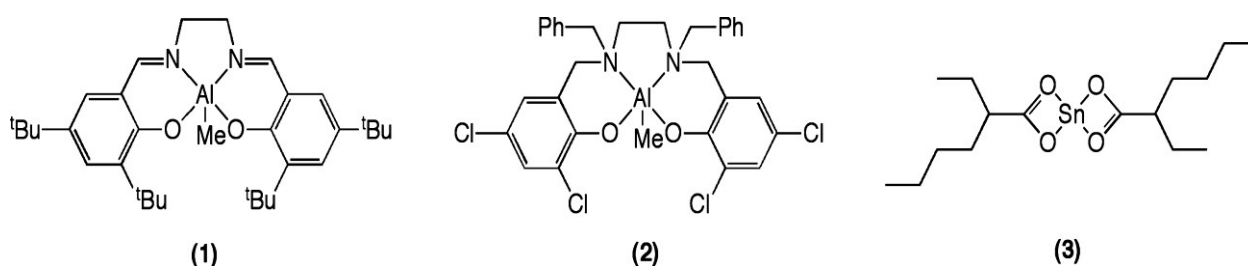
Figure 2. Catalyst precursors ᵗBu[salen]AlMe (**1**), ᶜˡ[salan]AlMe (**2**), and Sn(Oct)$_2$ (**3**).

To investigate systematically the effect of polymer tacticity on a family of PLA polymer stars, we attempted to develop a standardized synthetic procedure applicable to a wide array of catalyst systems. DPE was selected as the core initiator based on its inherent flexibility and successful use in tin(II)-catalyzed polymer star syntheses.[27] Initial attempts at preparing DPE−PLA polymer stars varied the standard procedure used for the aluminum-catalyzed ROP of *rac*-lactide.[30, 31] With the DPE core replacing traditional isopropanol or

benzyl alcohol initiators, standard conditions of a toluene solvent, 70 °C, and monomer/catalyst/alcohol functionality ratios of 60:1.2:1 were used. Under these conditions and regardless of the catalyst employed (1−3), bimodal distributions were observed upon analysis by GPC, with a significant low-molecular-weight fraction present. In addition, long initiation times were observed, especially with the aluminum-based catalysts. It was suspected that the low solubility of DPE in toluene, an issue noted previously,[26] was complicating this procedure. Attempts to prepare macroinitiators by refluxing the catalysts and DPE in toluene prior to monomer addition were unsuccessful.

To combat this low solubility, we pursued a synthetic protocol in neat, molten lactide in which DPE is freely soluble. By removing the toluene solvent and raising the reaction temperature to 120 °C, we observed monomodal GPC traces and minimized initiation times. This solvent-free synthetic procedure importantly improves the environmental impact of the biodegradable polymer generation following the principles of green chemistry.[35] In a representative reaction, as shown in eq 1, 60 equiv of rac-lactide, 1 equiv of DPE, and ~7 equiv of 1, 2, or 3 were added to an ampule under a N_2 atmosphere. These ratios were chosen to provide six-armed polymer stars with 10 monomer units per arm and at least one catalyst molecule per polymer arm. The ampules were sealed and transferred to a preheated (120 °C) oil bath to melt the lactide and promote the reaction. Polymerization of rac-lactide by catalysts 1 and 2 was significantly slower than that for 3, so reaction times were varied to keep % conversion consistent across all samples. Reaction times for catalysts 1−3 were 12, 18, and 4 h, respectively. After the allotted time period, the reactions were exposed to the atmosphere and quenched with MeOH or $PhCH_2OH$ in CH_2Cl_2 and then precipitated from cold methanol, collected, and dried in vacuo prior to analysis.
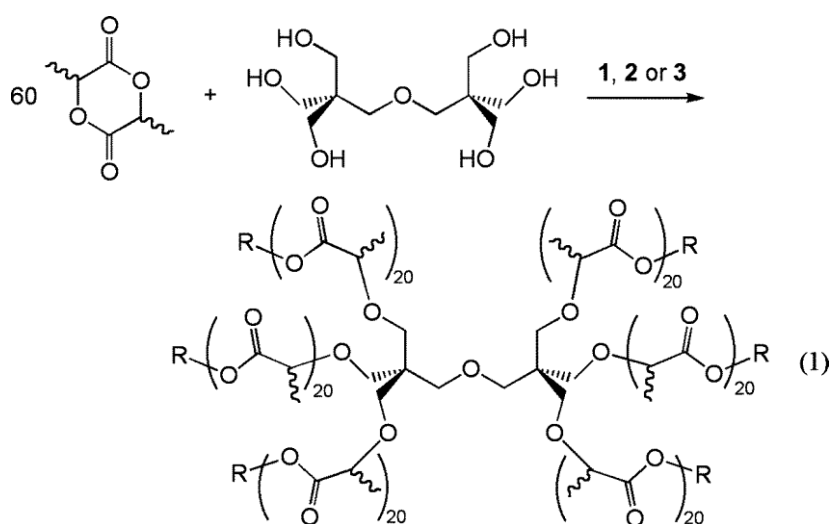
Analysis of these polymer stars by ^1H NMR spectroscopy provided information on the effective tacticity control offered during these reactions. In linear PLA systems, 1 showed a bias toward isotacticity (83%),[31]

whereas **2** showed a bias for heterotacticity (96%).[30] Solvent-free aluminum-catalyzed lactide polymerizations have surprisingly not appeared in the literature because of a presumed loss of stereoselectivity at the higher temperatures required for molten lactide reactions.[31] In the case of DPE polymer star synthesis, the tacticity control observed in linear polymer synthesis is maintained, even at these higher temperatures, as long as a high-quality inert atmosphere is maintained. Homonuclear decoupled ^{1}H NMR spectra of the methine region of PLA generated from *rac*-lactide, DPE, and **1**, **2**, and **3** showed tacticity biases of 85% isotactic, 80% heterotactic, and 100% atactic, respectively.

Varying the catalyst and monomer generates a family of DPE polymer stars, as shown in Table 1. For each tacticity type, two samples are reported to ascertain the effect of small differences in molecular weight on the thermal properties and to ensure that observed differences are due to tacticity changes. Monomer conversion was determined gravimetrically and used to calculate expected molecular weights ($M_{n,th}$). In most cases, these molecular weights matched well with those determined by GPC relative to polystyrene standards after application of a correction factor of 0.58.[36] The good correlation between these values suggests similar hydrodynamic volumes for the polymer stars and linear PLA chains. Longer star arms would be expected to deviate significantly in effective hydrodynamic volume.[37] Low polydispersity indices indicate good control over the polymerization reaction. Recognition of differences in the hydrodynamic volumes of PLA star polymers when compared with linear analogues led to verification of the polymer molecular weights by ^{1}H NMR spectroscopy of crude samples by integrating polymer peaks relative to ^{1}H chemical shifts from the polyolic DPE core. In all cases, molecular weights were within 10%, suggesting relatively small deviations for these short-armed star polymers. The disappearance of DPE resonances at δ 3.44 (OCH_2C(CH$_2$OH)$_3$) and δ 3.59 (OCH$_2$C(CH_2OH)$_3$) and the appearance of distinct, broadened polyol core peaks at δ 3.36 and 4.15 confirms activation of all six alcohol functionalities for each catalyst.

Table 1. Polymerization Data for DPE Poly(lactic acid) Polymer Stars

entry[a]	catalyst	monomer	tacticity bias	% conv.	$M_{n,GPC}$[b]	$M_{n,th}$	PDI	$Đ_{arm}$[c]
A-1	**3**	*rac*-LA	atactic	94	8873	9464	1.14	1.89
A-2	**3**	*rac*-LA	atactic	92	9058	9833	1.18	2.14
H-1	**2**	*rac*-LA	heterotactic	95	8440	8497	1.19	2.21
H-2	**2**	*rac*-LA	heterotactic	95	8755	8923	1.26	2.65
I-r-1	**1**	*rac*-LA	isotactic (*rac*)	92	8501	8639	1.22	2.40
I-r-2	**1**	*rac*-LA	isotactic (*rac*)	94	8688	8781	1.22	2.40
I-l-1	**3**	l-LA	isotactic (l)	99	8691	8781	1.08	1.51
I-l-2	**3**	l-LA	isotactic (l)	99	8771	8781	1.18	2.14

a Polymerization conditions: 60:1.2:1 monomer/catalyst/alcohol functionality.

b Molecular weights determined relative to styrene standards and corrected by 0.58 conversion factor.

c $Đ_{arm}$ calculated by Szymanski method.(38)

Thermal Properties of Tacticity Controlled Polymer Stars

Thermogravimetric analysis and DSC were used to study the physicochemical properties of star-shaped PLAs with various tacticities. TGA has been useful in assessing the properties of polymer stars, with previous reports indicating that for star-shaped PLA the maximum decomposition temperature (T_{max}), where polymer decomposition has ended, is lower than its linear analogues and that T_{max} is highly dependent on M_n with a decrease in molecular weight correlating to a lower T_{max}.(39) TGA data for polymer stars A-1 to I-l-2 inclusive are found in Table 2.

Table 2. TGA Data for PLA Star Polymers[a]

entry	onset (°C)	50% (°C)	T_{max} (°C)	ΔT_{decomp} (°C)
A-1	232.2	255.1	320.5	88.3
A-2	234.7	257.6	321.2	86.6
H-1	278.7	309.1	351.2	72.5
H-2	275.8	305.3	351.2	75.4
I-r-1	274.8	306.2	375.5	100.6
I-r-2	278.5	306.7	374.7	96.2
I-l-1	276.4	304.5	354.3	77.9
I-l-1	267.3	302.2	350.0	82.7

a Heating rate of 10 °C/min.

The introduction of stereocontrol has a large effect on the thermal stability of the polymers. Atactic PLA stars exhibit the lowest thermal stability of our samples at the onset of intense thermal decomposition (~230 °C), 50% sample decomposition (~255 °C), and maximum decomposition temperature (~320 °C). Onset temperatures for polymers with a specific tacticity bias show an enhancement in thermal stability of 40 °C regardless of the relative stereochemistry of the polymer chain or monomer used. In fact, the presence of unique tetrads (RRRR/SSSS in isotactic or RRSS in heterotactic) has little effect on either the onset or 50% decomposition temperatures. Differences are observed, however, in the T_{max} values. Heterotactic and isotactic-(l) polymer stars exhibit a stabilization of ~30 °C relative to the T_{max} of the corresponding atactic polymer star. Isotactic-(d/l) polymer stars, prepared from the relatively inexpensive *rac*-lactide, show a >50 °C increase in maximum thermal stability. The difference between the two isotactic polymer stars is especially noticeable and may be due to some stereocomplex behavior of adjacent polymer arms[40] or from stereoerrors resulting from the imperfect catalyst isospecificity.

These two effects manifest in a striking difference in the temperature window over which these polymer stars decompose with the ordered heterotactic and isotactic-(l) stars exhibiting relatively narrow decomposition profiles compared with isotactic-(d/l) PLA stars. An overlay of the TGA traces for four stars of various tacticities is shown in Figure 3 and provides further insight into this phenomenon. As can be seen, the

extended decomposition window arises from a small portion (<5%) of high thermal stability, and the majority of the isotactic-(d/l) decomposition occurs over a wider window than heterotactic and isotactic-(l) PLA stars. The effect of molecular weight on the decomposition temperatures appears minor, showing small differences in the onset temperatures.
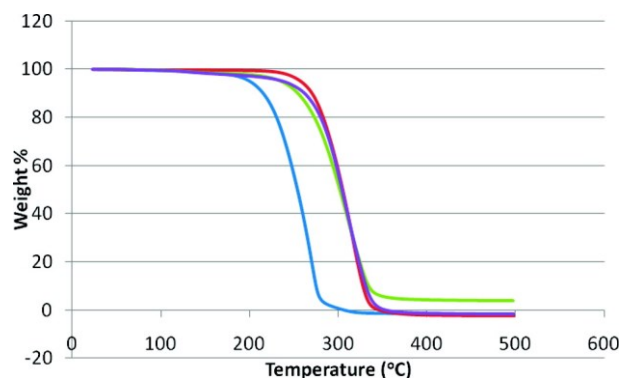

Figure 3. TGA overlay of star-shaped PLA possessing various tacticities. Blue = entry A-1, purple = H-1, green = I-r-1, red = I-l-1.

Beyond the thermal stability of the system, other thermal transitions were investigated by DSC. It is well-documented that the glass-transition temperatures (T_g), melting temperatures (T_m), and crystallinity of star-shaped PLAs are lower than their linear counterparts, but little information is available on the relationship between tacticity and these properties in polymer stars.(37) Table 3 shows that incorporating stereocontrol into PLA arms of star polymers has a significant effect on the T_g of the resulting polymer.

Table 3. DSC Thermal Transitions Observed for Star-Shaped PLAs of Different Tacticity Biases[ab]

entry	T_g (°C)	T_m (°C)	ΔH_m (J/g)	T_c (°C)
A-1	39.90			
A-2	37.29			
H-1	41.45			
H-2	41.52			
I-r-1	43.72	114.54, 134.41	24.8	84.19
I-r-2	43.26	117.18, 128.47	28.7	
I-l-1	47.67	131.96, 142.93	30.8	
I-l-2	48.24	122.91, 137.39	39.2	96.94

a Purge flow 50 mL/min N_2, heating/cooling rate 5 °C/min, heat (160 °C)/cool (0 °C)/heat (160 °C) cycle employed.

b For reference, linear isotactic, heterotactic, and atactic T_g values are 55−65, 40−45, and 53−54 °C, respectively.(41, 42)

Across all samples, the small molecular-weight differences observed impart little change to T_g values, with surprising consistency observed for heterotactic and isotactic samples. Atactic, heterotactic, and isotactic polymer stars all exhibit glass-transition temperatures, with clear differences observed for samples of different tacticities. Atactic PLA stars exhibit the lowest T_g, whereas purely isotactic stars derived from l-lactide possess the highest T_g. Interestingly, heterotactic and isotactic-(*rac*) stars possess a T_g between these two extremes, suggesting that the stereoerrors in the polymers produced from *rac*-lactide lower the temperature of the observed glass transitions. Variations in T_g for a subsection of PLA polymer stars are shown in Figure 4.
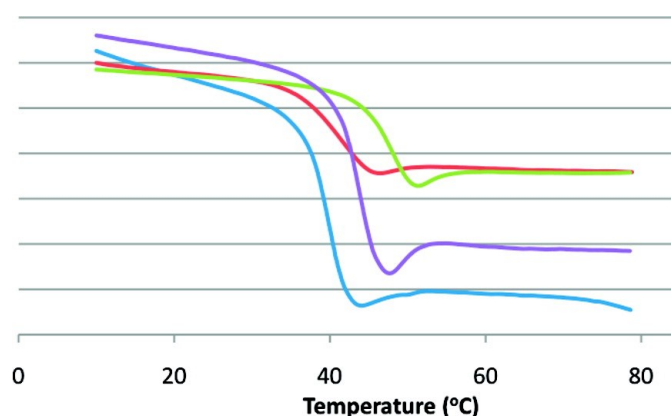

Figure 4. DSC overlay of T_g observed for star-shaped PLAs with various tacticity biases. Blue = entry A-1, purple = H-1, red = I-r-1, green = I-l-1.

Melting temperatures, in agreement with studies on linear PLA,[5] have been observed only for isotactic PLA stars. The lack of true melting signals for atactic PLA is in accord with its amorphous nature, whereas the lack of heterotactic PLA melting signals remains an unexplained artifact of its microstructure. The presence of two melting signals in isotactic samples is indicative of star-shaped PLAs, suggesting that the polymers are semicrystalline.[43-45]Differences in crystallite size and varying degrees of crystallinity within the polymer star sample create the two transitions. As was the case for T_g transitions, isotactic-(*rac*) T_m transitions are significantly lower than those for isotactic-(l) stars, suggesting that the T_m can be tuned by slight variations of the monomer composition or stereoerrors incorporated into the framework. The impact of these differences is mitigated slightly by significant differences observed between samples of varying molecular weights. Still, when comparing samples I-r-2 (8688 Da) and I-l-1 (8691 Da), the effect of utilizing *rac*-LA is clear. Crystallization temperatures were measured for select samples. Broad, lowered crystallization temperatures indicate that the materials can form highly crystalline segments, even at lower temperatures, supporting the possible presence of highly ordered stereocomplex segments. Representative DSC plots are shown in Figure 5.
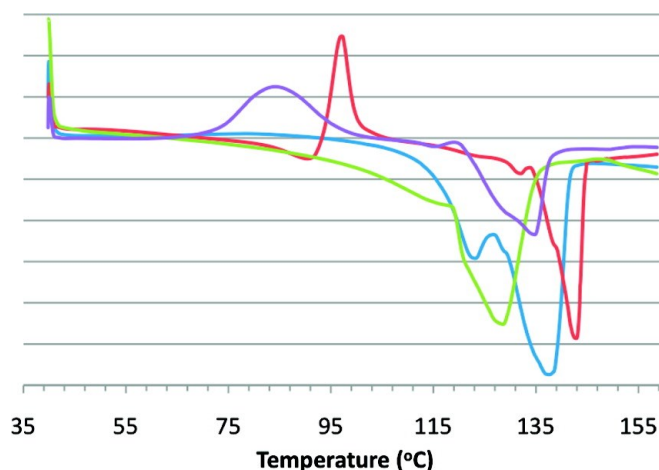
Figure 5. DSC overlay for star-shaped PLAs with an isotactic bias. Purple = entry A-1, green = H-1, red = I-r-1, blue = I-l-1.

The percent crystallinity was also calculated for isotactic samples from the theoretical ΔH_{fus} for idealized 100% crystalline PLA of 93.1 J/g.[46] In comparing these samples, we are examining their preferred crystalline form, so we have not subtracted the induced crystallinity observed from the T_c in samples I-r-1 and I-l-1 to more accurately represent trends in polymer star crystallinity. As expected, samples generated from pure l-lactide (three-sample average of 37%) possess higher % crystallinity than their *rac*-lactide counterparts (28%). The presence of stereoerrors may lower the ability of the polymer to form crystalline regions.

Crystallite Analysis by p-XRD

The semicrystalline natures of star-shaped PLAs were further investigated by p-XRD. Samples were prepared as solid pellets on glass substrates, and the Scherrer equation[47] was utilized to calculate crystallite size. These values are reported in Table 4.

Table 4. p-XRD Data for Polymer Stars[a]

entry	angle (deg)	crystallite size (nm)	*d* spacing (Å)
A-1			
A-2			
H-1			
H-2			
I-r-1	16.909	178	5.242
I-r-2	16.926	160	5.239
I-l-1	16.941	170	5.236
I-l-2	16.830	188	5.266

a Scherrer parameters: $K = 0.9$, $\lambda = 1.542$.

The angle of diffraction representing the crystalline regions of isotactic samples I-r-1, I-r-2, I-l-1, and I-l-2 is very consistent, adding further evidence of the strong isotactic bias imposed by catalyst **1**. Crystallite size is relatively consistent between isotactic samples. Figure 6, a collection of X-ray powder diffraction spectra, shows this trend more clearly. Spectra A and B, representing entries I-l-1 and I-r-1, respectively, show sharp diffraction peaks and small lower order diffraction peaks from crystalline regions superimposed over a broad sample baseline indicative of amorphous character. Finally, atactic and heterotactic PLA are shown in spectra C and D and are completely amorphous with no quantifiable reflections. No significant differences are observed in the X-ray powder patterns of samples possessing the same tacticity bias.
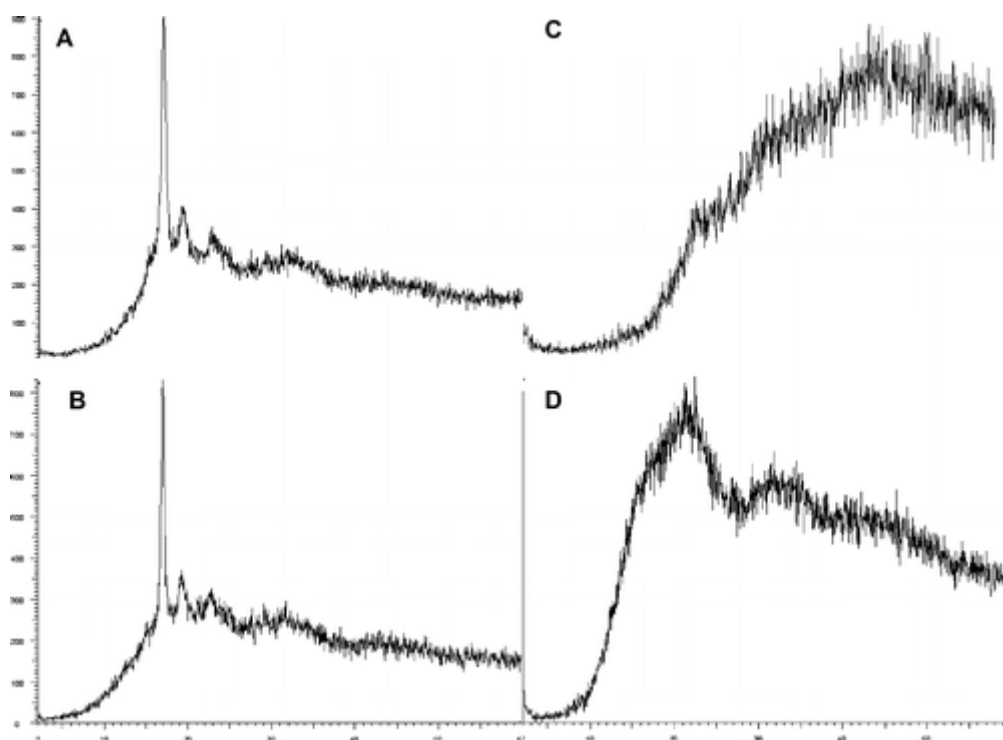

Figure 6. p-XRD analysis of star-shaped PLAs: (A) entry I-l-1, (B) I-r-1, (C) H-2, and (D) A-1.

Polymer Degradation

Pellets of atactic, heterotactic, isotactic-(*rac*), and isotactic-(l) PLA stars were prepared in a manual press and exposed to a 0.05% (w/v) solution of TBD (1,5,7-*triaza*-bicyclo[4.4.0]dec-5-ene) in methanol. This organic base has been shown to be highly successful in promoting the degradation of PLA materials into lactic acid via transesterification.[29] The time required for complete degradation and solvation of six pellets of each tacticity was recorded, and degradation was confirmed by both ^{1}H NMR spectroscopy and GPC analysis. Polymer stars with an atactic bias degraded fastest, in an average of 20.5 min. Heterotactic samples also

degraded quickly, with average lifetimes of 23.0 min. The short-lived nature of these heterotactic PLA samples agrees with reports on linear PLA homopolymers.[37] Little variation was observed between samples with slightly different molecular weights.

Surprisingly, significant differences were observed when examining the degradation of isotactic*rac*- and l-lactide-derived star polymers. Over a longer time frame, sample degradation times correlated to small differences in molecular weight. However, much greater differences were observed that correlated to the tacticity bias of the samples. In isotactic samples, ranging in M_n from 8.4 to 8.9 kDa, *rac*-PLA star degradation times varied from 51 to 66 min. These degradation rates appear to be two to three times faster for atactic samples versus isotactic samples derived from *rac*-LA. Further stability toward degradation was found in moving to isotactic-lPLA star polymers, where degradation times ranged from 167 to 184 min. The stereopure form persists for three times longer than that of isotactic samples derived from *rac*-LA, showing the dramatic effect of stereoerrors on the stability of the samples. One goal of this work was to pursue the quest of variable degradation rates by exploiting imperfect stereoregular polymerizations and to quantify the differences between isospecific polymer stars from different monomer feedstocks. In that regard, we are continuing to examine the tuning of degradation rates through controlling the percent isotacticity in polymer star samples.

Conclusions

Stereocontrolled star-shaped PLAs have been successfully synthesized by utilizing a series of aluminum and tin catalysts. These catalysts retain high activity in the activation of multifunctional initiators and are effective in polymerizing *rac*- and l-lactide in the molten state. PLA star polymers have been characterized by ^{1}H NMR, GPC, TGA, DSC, and p-XRD, and preliminary degradation studies have been performed. The introduction of stereocontrol has pronounced effects on the properties of star-shaped PLAs, manifesting in changes in thermal stability, T_m, T_g, crystallinity and solution stability, and polymer degradability. These differences dwarf those arising from differences in M_n or α-end group observed in previous studies. Importantly, significant differences exist between isotactic polymer stars derived from the two different monomer feedstocks, suggesting that stereoerrors can play a significant role in tuning these key physical parameters.

Notes and references

[1] Gunatillake, P.; Mayadunne, R.; Adhikari, R. *Biotechnol. Annu. Rev.* **2006**, 12, 301–347.

[2] Leenslag, J. W.; Goglewski, S.; Pennings, A. J. *J. Appl. Polym. Sci.* **1984**, 29, 2829–2842.

[3] Ishaug-Riley, S. L.; Crane-Kruger, G. M.; Yaszemski, M. J.; Mikos, A. G. *Biomaterials.* **1998**,19, 1405– 1412.

[4] Uhrich, K. E.; Cannizzaro, S. M.; Langer, R. S.; Shakesheff, K. M. *Chem. Rev.* **1999**, 99,3181– 3198.

[5] Stanford, M. J.; Dove, A. P. *Chem. Soc. Rev.* **2010**, 39, 486– 494.

[6] Kissel, T.; Li, Y. X.; Unger, F. *Adv. Drug Delivery Rev.* **2002**, 54, 99– 134.

[7] Wang, L.; Cai, C.; Dong, C.-M. *Chin. J. Polym. Sci.* **2008**, 26, 161– 169.

[8] Tomalia, D. A. *Prog. Polym. Sci.* **2005**, 30, 294– 324.

[9] Astruc, D.; Chardac, F. *Chem. Rev.* **2001**, 101, 2991– 3023.

[10] Li, Y. X.; Volland, C.; Kissel, T. *Polymer* **1998**, 39, 3087– 3097.

[11] Breitenbach, A.; Pistel, K. F.; Kissel, T. *Polymer* **2000**, 41, 4781– 4792.

[12] Cai, Q.; Zhao, Y.; Bei, J.; Xi, F.; Wang, S. *Biomacromolecules* **2003**, 4, 828– 834.

[13] Qinghui, H.; Faxue, L.; Qiaobo, L.; Yang, L.; Lin, J.; Jing, Y.; Qiang, F.; Amin, C.*Biomacromolecules.* **2005**, 6, 2236– 2247.

[14] Arvanitoyannis, I.; Nakayama, A.; Kawasaki, N.; Yamamoto, N. *Polymer* **1995**, 36, 2947–2956.

[15] Arvanitoyannis, I.; Nakayama, A.; Psomiadou, E.; Kawasaki, N.; Yamamoto, N. *Polymer***1996**, 37, 651– 660.

[16] Li, Y. X.; Nothnagel, J.; Kissel, T. *Polymer* **1997**, 38, 6197– 6206.

[17] Breitenbach, A.; Kissel, T. *Polymer* **1998**, 39, 3261– 3271.

[18] George, K. A.; Schue, F.; Chirila, T. V.; Wentrup-Byrne, E. *J. Polym. Sci., Part A: Polym. Chem.* **2009**, 47, 4736– 4748.

[19] Moravek, S. J.; Messman, J. M.; Storey, R. F. *J. Polym. Sci., Part A: Polym. Chem.* **2009**,47, 797– 803.

[20] Xie, Z.; Lu, C.; Chen, X.; Chen, L.; Wang, Y.; Hu, X.; Shi, Q.; Jing, X. *J. Polym. Sci., Part A: Polym. Chem.* **2007**, 45, 1737– 1745.

[21] Kricheldorf, H. R.; Ahrensdorf, K.; Rost, S. *Macromol. Chem. Phys.* **2004**, 205, 1602–1610.

[22] Kim, E. S.; Byoung, C.; Kim, S. H. *J. Polym. Sci., Part B: Polym. Phys.* **2004**, 42, 939–946.

[23] Aoyagi, T.; Miyata, F.; Nagase, Yu. *J. Controlled Release* **1994**, 32, 87– 96.

[24] Kim, S. H.; Han, Y. K.; Kim, Y. H.; Hong, S. I. *Makromol. Chem.* **1993**, 194, 3229–3236.

[25] Wang, L.; Dong, C.-M. *J. Polym. Sci., Part A: Polym. Chem.* **2006**, 44, 2226–2236.

[26] Stanford, M. J.; Dove, A. P. *Macromolecules.* **2009**, 42, 141– 147.

[27] Biela, T.; Duda, A.; Penczek, S. *Macromolecules.* **2006**, 39, 3710– 3713.

[28] Wischke, C.; Neffe, A. T.; Steuer, S.; Lendlein, A. *J. Controlled Release* **2009**, 138, 243–250.

[29] Joung, Y. K.; Lee, J. S.; Park, K. D.; Lee, S.-J. *Macromol. Res.* **2008**, 16, 66– 69.

[30] Hormnirun, P.; Marshall, E. L.; Gibson, V. C.; White, A. J. P.; Williams, D. J. *J. Am. Chem. Soc.* **2004**, 126, 2688– 2689.

[31] Hormnirun, P.; Marshall, E. L.; Gibson, V. C.; Pugh, R. I.; White, A. J. P. *Proc. Natl. Acad. Sci. U.S.A.* **2006**, 103, 15343– 15348.

[32] Jerome, C.; Lecomte, P. *Adv. Drug Delivery Rev.* **2008**, 60, 1056– 1076.

[33] Nakano, K.; Kosaka, N.; Hiyama, T.; Nozaki, K. *J. Chem. Soc., Dalton Trans.* **2003**, 4039–4050.

[34] Tsuji, H. *Macromol. Biosci.* **2005**, 5, 569– 597.

[35] Anastas, P. T.; Warner, J. C. *Green Chemistry: Theory and Practice*; Oxford University Press: New York, **1998**; p 30.

[36] Kowalski, A.; Duda, A.; Penczek, S. *Macromolecules* **1998**, 31, 2114– 2122.

[37] Cameron, D. J. A.; Shaver, M. P. *Chem. Soc. Rev.* **2010**, ASAP. DOI:10.1039/c0cs00091d

[38] Szymanski, R. *Macromolecules* **2002**, 35, 8239– 8242.

[39] Zhao, Y. L.; Cai, Q.; Jiang, J.; Shuai, X. T.; Bei, J. Z.; Chen, C. F.; Xi, F. *Polymer* **2002**, 43,5819– 5825.

[40] Ikada, Y.; Jamshidi, K.; Tsuji, H.; Hyon, S. H. *Macromolecules* **1987**, 20, 904– 906.

[41] Henton, D. E.; Gruber, P.; Lunt, J.; Randall, J. Polylactic Acid Technology. In *Natural Fibres, Biopolymers, and Biocomposites*; Taylor and Francis Group: New York, **2005**.

[42] Becker, J. M.; Pounder, R. J.; Dove, A. P. *Macromol. Rapid Commun.*, published online July 8, http://dx.doi.org/10.1002/marc.201000088.

[43] Cohn, D.; Younes, H.; Marom, G. *Polymer* **1987**, 28, 2018– 2022.

[44] Migliaresi, C.; De Lollis, A.; Fambria, L.; Cohn, D. *Clin. Mater.* **1991**, 8, 111– 118.

[45] Hoogsteen, W.; Postema, A. R.; Pennings, A. J.; Ten Brinke, G.; Zugenmaier, P.*Macromolecules* **1990**, 23, 634– 642.

[46] Drumwright, R. E.; Gruber, P. R.; Henton, D. E. *Adv. Mater.* **2000**, 12, 1841–1846.

[47] Patterson, A. L. *Phys. Rev.* **1939**, 56, 978– 982.